Design and Experimental Analysis of a Fractional-Order Integral Controller for a Decoupled TITO Coupled Tank System

Chahira Boussalem[1,2], Fouad Yacef[2], Laid Degaa[3], Mahmoud Belhocine[2] and Nassim Rizoug[3]

***Abstract*—The significance of Bodes Ideal Transfer Function (BITF) in control theory has motivated researchers to explore new ways to harness its beneficial properties. In this work, we present a novel control strategy that integrates Input-Output Feedback Linearization (IOFL) with a Fractional Integral Controller (FIC) to achieve enhanced system performance. The proposed approach is applied to a Two-Input Two-Output (TITO) nonlinear system, where IOFL is first utilized to linearize and decouple the system into two independent pure integrator subsystems. Subsequently, a newly designed fractional-order integral controller, based on BITF, is implemented to ensure precise reference tracking. To validate the effectiveness of this method, we apply it to a TITO coupled tank (TITOCT) process and compare its performance with Nonlinear Continuous-Time Generalized Predictive Control (NCGPC).**

***Index Terms*—fractional controllers design, nonlinear systems, two input two output coupled tank system, Bode's ideal transfer function.**

I. Introduction

The design and application of fractional-order controllers remain a crucial area in control systems due to their ability to achieve high precision and robustness. However, the wide variety of available controllers often leads to challenges in selecting the most appropriate one. Researchers typically seek controllers that are both robust and minimal in terms of parameter complexity. Among the various fractional-order controllers, the fractional-order proportional-integral-derivative (FOPID) family has gained significant attention for its industrial applications. Several studies have explored different FOPID designs, including standard FOPID controllers [1], robust FOPID controllers [2-4], adaptive FOPID controllers [5], fractional-order proportional-derivative (FOPD) controllers [6], fractional-order proportional-integral (FOPI) state feedback controllers [7, 8], and robust FOPI controllers [9].

Most real-world systems exhibit nonlinear behavior, and many industrial processes belong to the category of multi-input multi-output (MIMO) systems. In MIMO control, numerous approaches rely on decoupling techniques [10,11], while others are based on feedback linearization [12,13]. In the case of two-input two-output (TITO) nonlinear systems, feedback linearization not only compensates for system nonlinearities but also decouples and transforms the system into independent single-input single-output (SISO) linear subsystems. This work aims to develop a novel approach for determining the integral gain of a fractional controller in TITO nonlinear systems to achieve accurate reference tracking, ensure robustness, and validate the method through implementation on a hydraulic system. Our approach integrates input-output feedback linearization (IOFL) with a fractional integral controller (FIC), imposing the closed-loop characteristic polynomial of Bodes Ideal Transfer Function (BITF) as the desired model. To the best of our knowledge, no existing work on TITO system control has explicitly addressed this problem. Moreover, very few studies have utilized the closed-loop transfer function (CLTF) of BITF as a reference model, as proposed in [14,15].

To validate the theoretical findings, we implement the proposed method on a nonlinear TITO coupled tank (TITOCT) experimental testbed. In integer-order control, various strategies have been employed for this system, including proportional-integral (PI) controllers [16] and other control techniques [17,18]. More recently, researchers have explored fractional-order controllers, such as a novel frequency-domain-based FOPI controller [19], an auto-tuning FOPI controller [20], and a semi-analytical approach for FOPID controller design [21].

Our main contributions are:

- Develop a novel fractional integral control method for a decoupled TITO nonlinear system to achieve accurate reference tracking;
- Ensure robustness by imposing BITF as the reference model
- Validate the proposed approach through simulations on a decoupled TITO process, followed by experimental implementation.
- Demonstrate the effectiveness of the method by comparing it with the robust nonlinear continuous-time generalized predictive control (NCGPC) strategy..

This paper is structured as follows: Section 2 presents the Coupled Two-Tank Modeling. Section 3 presents Input-Output Feedback Linearization of the Coupled Two-Tank Model. The design of a FPIC for double integrating systems is presented in Section 3. Section 4 presents the simulation and experimental

[1]Chahira Boussalem is with Automatic Department, University of Tizi-Ouzou, Algeria chahiraboussalem@gmail.com

[2]Chahira Boussalem, Fouad Yacef and Mahmoud Belhocine are with Centre de développement des technologies avancées CDTA, Algiers, Algeria chahiraboussalem@gmail.com, fyacef@cdta.dz, mbelhocine@cdta.dz

[3]Nassim Rizoug and Laid Degaa are with école Supérieure des Techniques Aéronautiques et de Construction Automobile ESTACA, Montigny-le-Bretonneux, France nassim.rizoug@estaca.fr, laid.degaa@estaca.fr

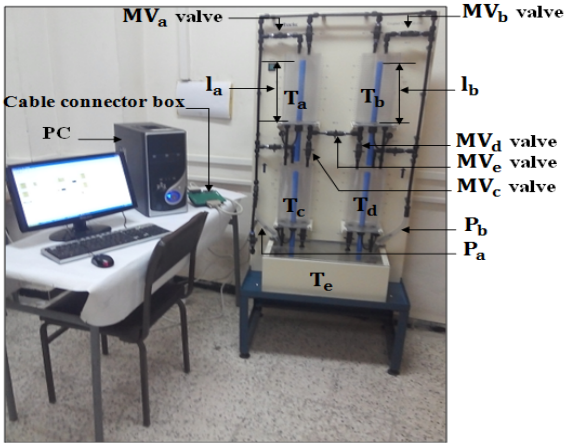

Fig. 1. Coupled tanks experimental testbed

results of the proposed method. We finish with a conclusion in Section 5.

II. Input Output Feedback Linearization Applied to Two-input Two-output Coupled Tank Process.

The coupled tank experimental testbed is a nonlinear system consisting of five tanks: four upper tanks with uniform cross-sections (denoted as M), placed on a platform, and a fifth tank positioned below them. In this study, we focus on the two upper tanks. Pump P_a supplies water to the upper tank (T_a) through the valve MV_adelivering a flow rate ϕ_a. Similarly, pump P_b supplies water to tank (T_b) through the valve MV_b with a flow rate ϕ_b. Additionally, tank (T_b) receives water from tank T_a via the valve MV_e and orifices of area e_{ab} contributing an additional flow ϕ_{ab}. Water exits tanks T_a and T_b through orifices with areas e_a and e_b, resulting in outflows ϕ_{ae} and ϕ_{be} respectively. The system inputs are the pump voltages u_a and u_b while the outputs are the water levels l_a and l_b in tanks T_a and T_b, respectively. The schematic of the experimental setup is shown in Figure 1.

The nonlinear state equation governing the dynamics of the coupled tank system is given in [16].

$$\begin{cases} \frac{dl_a}{dt} = \frac{\eta}{M}u_a - \frac{e_a}{M}\sqrt{2gl_a} - \frac{e_{ab}}{M}\sqrt{2g(l_a - l_b)} \\ \frac{dl_b}{dt} = \frac{\eta}{M}u_b + \frac{e_{ab}}{M}\sqrt{2g(l_a - l_b)} - \frac{e_b}{M}\sqrt{2gl_b}. \end{cases} \quad (1)$$

Let $x = [l_a, l_b]$ denote the state vector, $u = [u_a, u_b]$ the control vector, and $y = [y_a, y_b] = [l_a, l_b]$ the output vector. Assuming $e_a = e_b = e_{ab} = e$ and $\frac{\eta}{M} = \delta$. the state-space model of the TITOCT system is given by:

$$\begin{cases} \frac{dl_a}{dt} = \delta u_a - \frac{e}{M}\sqrt{2gl_a} - \frac{e}{M}\sqrt{2g(l_a - l_b)} \\ \frac{dl_b}{dt} = \delta u_b + \frac{e}{M}\sqrt{2g(l_a - l_b)} - \frac{e}{M}\sqrt{2gl_b} \\ y_a = l_a \\ y_b = l_b. \end{cases} \quad (2)$$

The numerical parameters of the two-input, two-output (TITO) coupled tank system are as follows: $M = 0.01389m^2$ represents the cross-sectional area of the tank, $e = 50.265.10^{-6}m^2$ is the outlet area of the tank, $\delta = 2.4.10^{-3}$ is the constant that relates the control voltage to the water flow from the pump. The gravitational acceleration is given by $g = 9.81ms^{-2}$ [22, 24].

The coupled tank system is modeled as a TITO nonlinear process, expressed in the following form:

$$\begin{cases} f(x) = \begin{bmatrix} f_a \\ f_b \end{bmatrix} \\ = \begin{bmatrix} -\frac{e}{M}\sqrt{2gl_a} - \frac{e}{M}\sqrt{2g(l_a - l_b)} \\ \frac{e}{M}\sqrt{2g(l_a - l_b)} - \frac{e}{M}\sqrt{2gl_b} \end{bmatrix} \\ g(x) = \begin{pmatrix} \delta & 0 \\ 0 & \delta \end{pmatrix}. \end{cases} \quad (3)$$

Let $r_i, i = 1, 2$, denote the relative degrees of the output $l_i, i = a, b$. The first derivative of each output is given by:

$$\dot{y}_{j,j=a,b} = L_f l_j(x) + \sum_{i=a}^{b}(L_{g_i} l_j)u_i = f_j + \delta u_j. \quad (4)$$

The input appears after the first derivative of each output y_j, hence the relative degree associated with $l_j, j = a, b$ is $r_j = 1$.

The system's vector relative degree is $(r_1, r_2) = (1, 1)$, meaning that the sum $(r_1 + r_2)$ equals the system order. Consequently, the system can be exactly feedback linearized, resulting in the absence of zero dynamics.

The nonlinear model described in (2) can be linearized using the state transformation [23]:

$$\begin{bmatrix} z_a \\ \cdots \\ z_b \end{bmatrix} = \begin{bmatrix} l_a \\ \cdots\cdots\cdots \\ l_b \end{bmatrix}, \quad (5)$$

and the corresponding feedback control laws [23]:

$$\begin{bmatrix} u_a \\ u_b \end{bmatrix} = \begin{bmatrix} L_{g_1}L_f^{r_1-1}l_a & L_{g_2}L_f^{r_1-1}l_a \\ L_{g_1}L_f^{r_2-1}l_b & L_{g_2}L_f^{r_2-1}l_b \end{bmatrix}^{-1}$$
$$\begin{bmatrix} -L_f^{r_1}l_a + \upsilon_a \\ -L_f^{r_2}l_b + \upsilon_b \end{bmatrix} = \begin{bmatrix} \frac{1}{\delta} & 0 \\ 0 & \frac{1}{\delta} \end{bmatrix}\begin{bmatrix} -f_a + \upsilon_a \\ -f_b + \upsilon_b \end{bmatrix}, \quad (6)$$

where υ_a and υ_b, are the control laws responsible for stabilizing each linear subsystem.

Finally, the overall control law is given by:

$$\begin{cases} u_a = \frac{1}{\delta}[\frac{e}{M}\sqrt{2gl_a} + \frac{e}{M}\sqrt{2g(l_a - l_b)} + \upsilon_a] \\ u_b = \frac{1}{\delta}[-\frac{e}{M}\sqrt{2g(l_a - l_b)} + \frac{e}{M}\sqrt{2gl_b} + \upsilon_b]. \end{cases} \quad (7)$$

In the new coordinates, the system is represented by:

$$\begin{cases} \begin{bmatrix} \dot{z}_a \\ \cdots \\ \dot{z}_b \end{bmatrix} = \begin{bmatrix} f_a + \delta u_a \\ \cdots\cdots\cdots\cdots \\ f_b + \delta u_b \end{bmatrix}, \\ y_a = z_a \\ y_b = z_b. \end{cases} \quad (8)$$

Remark: The output vector $y = [y_a, y_b]$ retains the same notation in both the original and transformed coordinate systems.

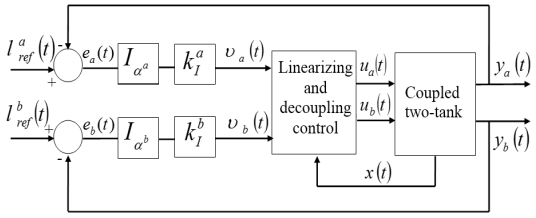

Fig. 2. Block diagram of IOFL with FIC in the decoupled TITO system

Substituting (7) into (8) results in two decoupled linear subsystems.

$$\begin{cases} \dot{z}_i = \upsilon_i \\ y_i = z_i \end{cases} \quad i = a,\ b, \tag{9}$$

.

III. Fractional Controller Design

The fractional integral controller design for the SISO system presented in [24] can be extended to decoupled TITO systems. The key idea behind using the fractional-order integral controller alone is that the controlled system behaves as a pure integrator. In fact, the combination of these two systems results in the Bode ideal transfer function in the closed-loop. We implement the fractional integral state feedback in the following form:

Let $\upsilon_i(t)$ be the proposed fractional integral state feedback controller of the following form

$$\begin{aligned} \upsilon_i(t) &= k^i_I I_{\alpha^i}(l^i_{ref}(t) - z_i) \\ &= k^i_I I_{\alpha^i}(l^i_{ref}(t) - y_i(t)),\ i = a,\ b, \end{aligned} \tag{10}$$

where $k^i_I \in R$, are the controllers gains. I_{α^i} are the fractional integration operators of order α^i. l^i_{ref} are the desired setpoint.

Let $e_i(t) = l^i_{ref} - y_i(t)$ be the error between the desired setpoint and the output. The block diagram of the IOFL with the FIC applied to the TITOCT process is illustrated in Figure 2.

The following algorithm outlines the steps for designing the fractional integral controller (FIC) described above:

Step 1: Apply IOFL to the TITO nonlinear system to obtain two first-order subsystems.

Step 2: Select the desired phase margin (or fractional order γ^i) and the gain crossover frequency of the desired closed-loop transfer function (CLTF), considering only values within the range $(1 < \gamma^i < 2)$ into consideration.

Step 3: Determine the controller parameters α^i and k^i_I using equation (13). These steps are applied separately to each first-order SISO subsystem.The detailed calculation of the fractional corrector is presented as follows. Let T_{cl} be the resulting CLTF from equations (9) and (10).

$$T_{cl} = \frac{z_i(s)}{l^i_{ref}(s)} = \frac{y_i(s)}{l^i_{ref}(s)} = \frac{k^i_I}{s^{\alpha^i+1} + k^i_I}. \tag{11}$$

T_{cl} is similar to an ideal tansfert function (the CLTF of the BITF) given in [14] by: $F_{Bode} = \frac{{\omega_c}^\gamma}{s^\gamma + {\omega_c}^\gamma}$, (where $\gamma = \alpha^i + 1$).

Let ω^i_c and γ^i be the desired gain crossover frequency and the fractional order of the closed loop reference for each subsystem i.

The desired closed loop reference is then

$$\Delta^i_d(s) = \frac{(\omega^i_c)^{\gamma^i}}{s^{\gamma^i} + (\omega^i_c)^{\gamma^i}}. \tag{12}$$

The term-by-term differentiation between the denominator of (11) and the denominator of (12), gives:

$$\begin{cases} k^i_I = (\omega^i_c)^{\gamma^i} \\ \alpha^i = \gamma^i - 1 \end{cases} \tag{13}$$

IV. Application and Comparative Study between the proposed method and NCGPC

In the present section, we provide a series of simulations followed by experimental implementation for step and square references to TITOCT system and a comparative study between the performances of the proposed control strategy and NCGPC of [25, 26].

A. Simulation Results

For both controllers, simulations are conducted using the initial conditions $l_a = 0$ and $l_b = 0$. Following Step 1 from Section 3, we derive the linear subsystems of the TITOCT system given by (9). Two different step reference tests are performed. In the first test, for the first subsystem, we fix the gain crossover frequency at $\omega^a_c = 0.08$ and vary either the phase margin $\Phi M^a = 72°, 54°, 36°$ or the fractional order γ^a as $\gamma^a = 1.2, 1.4, 1.6$. The corresponding controller gains are:
$\gamma^a = 1.2 \mapsto$ is chosen as 1.2, the controller gain is $k^a_I = [0.0483]$.
$\gamma^a = 1.4$, the controller gain is $k^a_I = [0.0291]$.
$\gamma^a = 1.6$, the controller gain is $k^a_I = [0.0176]$.
In the second test, for the second subsystem, we fix the fractional order at $\gamma^b = 1.1$ $(\Phi M^b = 81°)$ and vary the gain crossover frequency ω^b_c as $\omega^b_c = 0.2, 0.3, 0.5$. The corresponding controller gains are:
$\omega^b_c = 0.2$, the controller gain is $k^b_I = [0.1703]$.
$\omega^b_c = 0.3$, the controller gain is $k^b_I = [0.266]$.
$\omega^b_c = 0.5$, the controller gain is $k^b_I = [0.4665]$.

For NCGPC, simulation results illustrate the effect of predictive time T, using different values:
- $T^a = [0.5, 1.5, 3]$, for the first subsystem
- $T^b = [0.9, 2, 4]$, for the second subsystem. The system responses for these tests are shown in Figures 3 4,5 and 6.

Figures 3 and 4 show that, under the proposed controller, the output l_a tracks l^a_{ref} with varying overshoots but an almost constant rise time as γ^a changes while keeping ω^a_c fixed. Conversely, varying ω^b_c while maintaining a fixed γ^b, causes l_b to tracks l^b_{ref} with different rise times but a constant overshoot, demonstrating the iso-damping property. The proposed controller thus allows both ω^i_c and γ^i to influence system

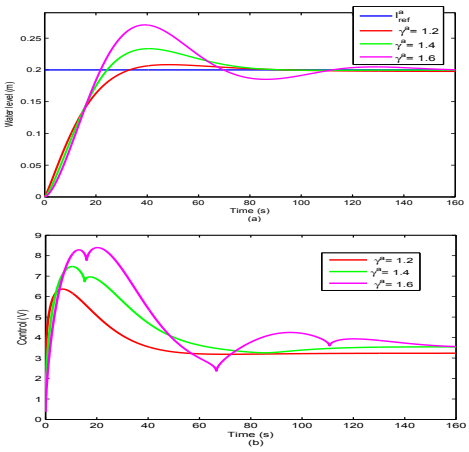

Fig. 3. Step response by using FL combined with FIC with different values of the fractional order γ, applied to the first subsystem: (a): Output response, (b): Control

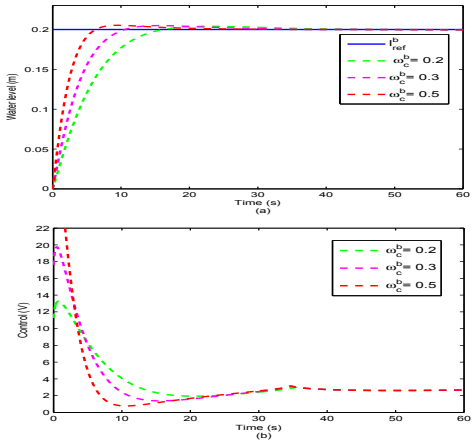

Fig. 4. Step response by using FL combined with FIC with different values of the gain crossover frequency ω_c, applied to the second subsystem: (a): Output response, (b): Control

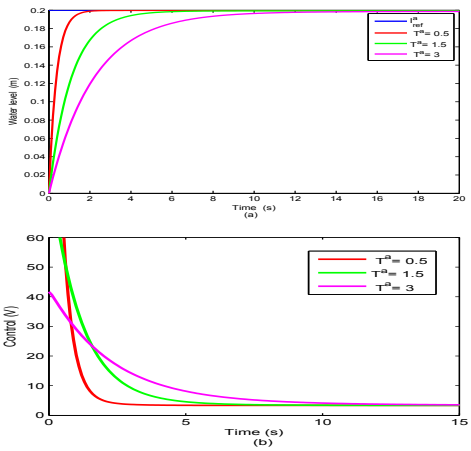

Fig. 5. Step response by using NCGPC with different values of the predictive time T, applied to the first subsystem: (a): Output response, (b): Control

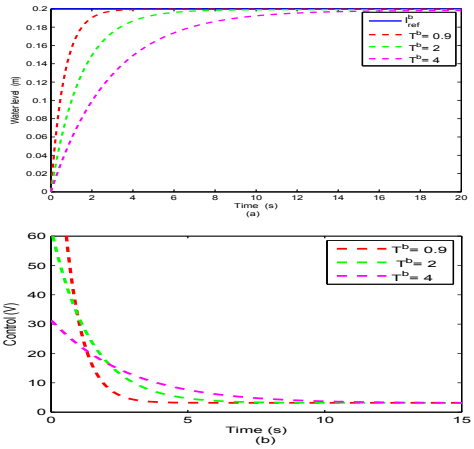

Fig. 6. Step response by using NCGPC with different values of the predictive time T, applied to the second subsystem: (a): Output response, (b): Control

dynamics. Figures 5 and 6 illustrate that for NCGPC, the system dynamics are affected by the choice of predictive time T^i.

For tracking desired vector outputs $[l^a_{ref}, l^b_{ref}]$ which are square signals, we apply the proposed fractional integral controller combined with feedback linearization and NCGPC to the vector outputs $[l_a, l_b]$ for each subsystem.

For the first controller:

• In the first subsystem, we set the fractional order to $\gamma^a = 1.1$ $(\Phi M^a = 81°)$ and the gain crossover frequency to $\omega^a_c = 0.08$.

•In the second subsystem, we set the fractional order to $\gamma^b = 1.1$ $(\Phi M^b = 81°)$ and the gain crossover frequency to $\omega^b_c = 0.3$.

For the second controller, simulation results are obtained using a fixed predictive time:

• $T^a = 0.5$ for the first subsystem. • $T^b = 0.1$ for the second.

The simulation results for these tests are illustrated in Figures 7 and 8.

It can be seen from Figures 7 and 8 controllers ensure that the first output, l_a accurately tracks the setpoint l^a_{ref} while the second output, l_b tracks the setpoint l^b_{ref} rapidly and with zero steady-state error. The water levels are well-tracked with an acceptable control effort.

B. Experimental Results

For the proposed controller, experimental results are given for a square reference, and for the same initial conditions and the same controllers parameters as that of simulation. This test is illustrated in Figures 9 and 10. The latters show that the proposed controller can properly achieve reference tracking.

To further evaluate the robustness of the proposed controllers, we introduced two external disturbances in the experimental testbed, as illustrated in Figures 11 and 12. The first disturbance involved adding one liter of water to Tanks 1 and 2 at $t = 250s$ and $t = 350s$, respectively. The second disturbance was induced by opening the MV_c and MV_d valves at $t = 100s, 560s, 670s$ and $t = 100s, 670s$, respectively,

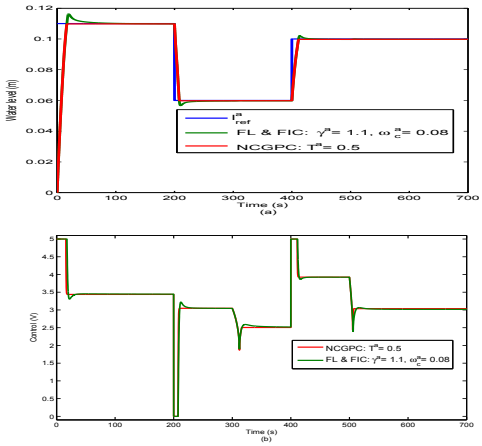

Fig. 7. Simulation results for a square reference using FL combined with FIC and NCGPC, applied to the first subsystem, (a): Output response, (b): Control

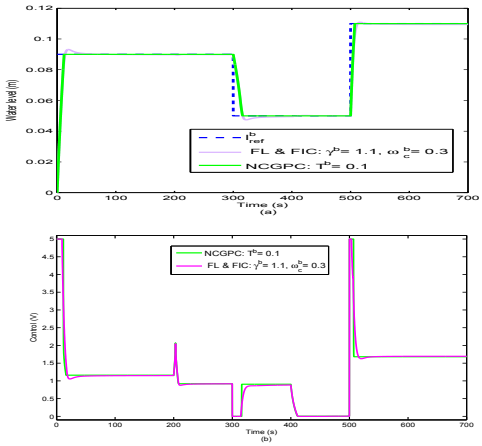

Fig. 8. Simulation results for a square reference using FL combined with FIC and NCGPC, applied to the first subsystem, (a): Output response, (b): Control

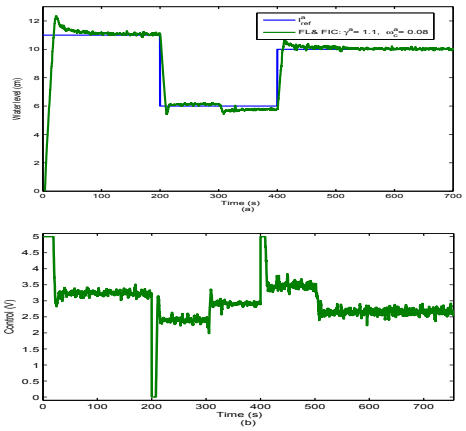

Fig. 9. Experimental results for square reference without disturbance, using FL combined with FIC, applied to the first subsystem, (a): Output response, (b): Control

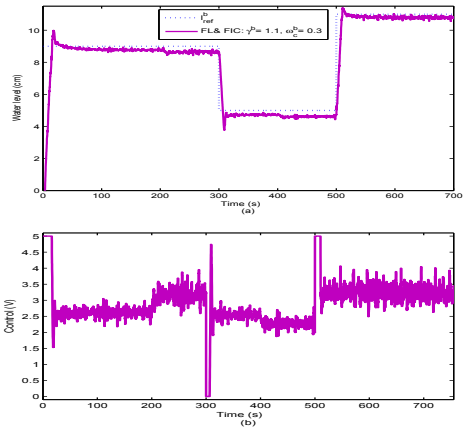

Fig. 10. Experimental results for square reference without disturbance, using FL combined with FIC, applied to the second subsystem, (a): Output response, (b): Control

for a few seconds. The controller is tested using the same parameters as in the no-disturbance test .

Figures 11 and 12 show that after the first external disturbance, the water level increases instantly, and then it is decreased, achieving the reference value. After the second external disturbance, the water level decreases, and then it is increased, achieving the reference value.

V. Conclusion

This manuscript introduces a novel reference-tracking technique for a TITO nonlinear system by integrating IOFL and FIC. The latter's design is simplified using BITF as the reference model, ensuring closed-loop stability and robustness. Two key parameters, the gain crossover frequency ω_c^i and the fractional order γ^i) influence the system's dynamics. Meanwhile, NCGPC, an optimal control strategy, determines controller gain coefficients by minimizing the criterion J. The system dynamics vary with predictive times T^i. an increase in predictive times extends the rise time while reducing control effort. A comparison of simulation results demonstrates that both controllers exhibit excellent tracking performance and robustness. These results confirm the effectiveness of the proposed controller.

dci Authors declared no potential conflicts of interest with respect to the research, authorship, and publication of this article.

funding Authors received no financial support for the research, authorship, and publication of this article.

References

[1] Maheswari C., Priyanka EB and Meenakshipriya B. Fractional-order $PI^{\lambda}D^{\mu}$ controller tuned by coefficient diagram method and particle swarm optimization algorithms for SO2 emission control process. *Proc IMechE, Part I: J Systems and Control Engineering* 2017; 231: 587–599.

[2] Beschi M., Padula f. and Visioli A. The generalized isodamping approach for robust fractional PID controllers design. *International Journal of Control* 2015; 90: 1157–1164.

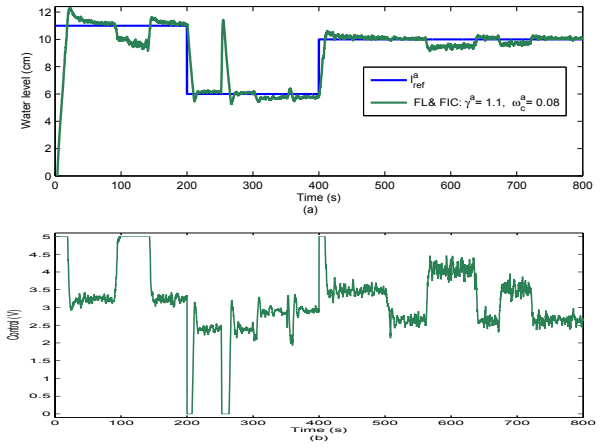

Fig. 11. Experimental results with external disturbance, using FL combined with FIC, applied to the first subsystem, (a): Output response, (b): Control

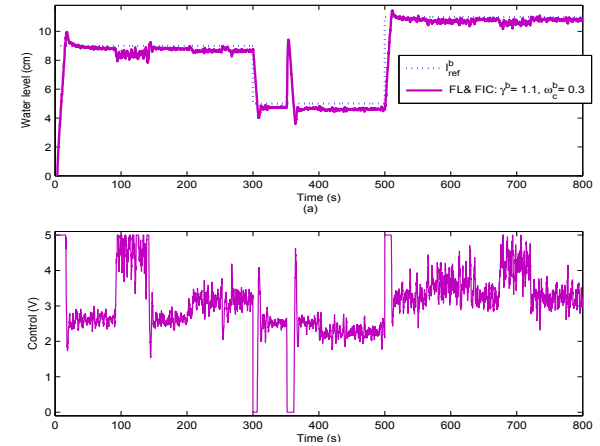

Fig. 12. Experimental results with external disturbance, using FL combined with FIC, applied to the second subsystem, (a): Output response, (b): Control

[3] Hamidian H. and Beheshti MTH. A robust fractional-order PID controller design based on active queue management for TCP network. *International Journal of Systems Science* 2018; 49: 211–216.

[4] Damarla SK and Kundu M. Design of robust fractional PID controller using triangular stript operational matrices. *Fractional calculus and applied analysis, an international journal or theory and applications* 2015; 18: 1291–1326.

[5] Yaghooti B. and Salarieh H. Robust adaptive fractional order proportional integral derivative controller design for uncertain fractional order nonlinear systems using sliding mode control. *Proc IMechE, Part I: J Systems and Control Engineering* 2018; 232: 550–557

[6] Zhang L., Liu L. and Zhang S. Design, Implementation, and Validation of Robust Fractional-Order PD Controller for Wheeled Mobile Robot Trajectory Tracking. *Complexity* 2019; 2020: 1–12.

[7] Bettayeb M., Boussalem C., Mansouri R. et al. Stabilization of an inverted pendulum cart system by fractional PI State feedback. *ISA Transactions* 2014; 53: 508–516

[8] Mansouri R., Bettayeb M., Boussalem C. et al. Linear integer order system control by fractional PI- state feedback', *Fractional Calculus Applications*, Abi Zeid Daou, R. and Moreau, X., Nova Science Publishers, New York, 2015, pp.65–91

[9] Azarmi R., Tavakoli-Kakhki M., Sedigh AK et al. Robust Fractional Order PI Controller Tuning Based on Bode's Ideal Transfer Function. *IFAC-PapersOnLine* 2016; 49: 158–163.

[10] Gagnon E., Pomerleau A., Desbiens A. Simplified, ideal or inverted decoupling. *ISA Transactions* 1998; 37: 265–276.

[11] Zhang S., Zhu Y., Mu H. et al. Decoupling and levitation control of a six-degree-of-freedom magnetically levitated stage with moving coils based on commutation of coil array. *Proc IMechE, Part I: J Systems and Control Engineering* 2012; 226: 875–886.

[12] Zhang J., Yang W. and Feng P. A feedback linearization controller combined with a data-driven subspace-based prediction method for vehicle handling stabilization. *Proc IMechE, Part I: J Systems and Control Engineering* 2018; 233: 1156–1180.

[13] Ur Rehman O., Petersen IR and Fidan B. Feedback linearization-based robust nonlinear control design for hypersonic flight vehicles. *Proc IMechE, Part I: J Systems and Control Engineering* 2012; 227: 3–11.

[14] Barbosa R., Machado JAT and Sneddon IN. Tuning of PID controllers based on Bode's ideal transfer function. *Nonlinear Dynamics* 2004, 305–321.

[15] Al-Saggaf UM, Mehedi IM, Mansouri R. et al. State feedback with fractional integral control design based on the Bode's ideal transfer function. *International Journal of Systems Science* 2015, 1–13.

[16] Gurumurthy G and Das DK. Proportional-Integral (PI) Controller Design and Implementation for Decoupled Two-Input Two-Output-Coupled Tank System with Dead-time. In: *2019 Sixth Indian Control Conference (ICC)*, India, December 18-20 2019, pp.502-507.

[17] Abdalla AN, Ibrahim TK and Tao H. Adaptive Fuzzy / PD controller for Coupled Two Tank Liquid Levels system. In: *MATEC Web of Conferences*.PP.1–9.

[18] Nurnsomrarr A., Suksri T. and Thumma M. Design of 2-DOF PI Controller with Decoupling for Coupled-Tank Process. In: *COEX, International Conference on Control , Automation and Systems*, Seoul, Korea, 17-20 Oct 2007, pp.339–344.

[19] Gurumurthy G and Das DK. An $FO-[PI]^{\lambda}$ controller for inverted decoupled two-input two-output coupled tank system. *International Journal of Systems Science* 2018, 392–402.

[20] Baruah G., Majhi S. and Mahanta C. Auto-tuning of FOPI controllers for TITO processes with experimental validation. *International Journal of Automation and Computing* 2018; 16: 589–60.

[21] Gurumurthy G. and Das DK. A Semi-Analytical Approach to Design a Fractional Order Proportional-Integral-Derivative (FOPID) Controller for a TITO Coupled Tank System. In: *Proportional-Integral-Derivative (FOPID) Controller for a TITO Coupled Tank System, 2019 IEEE Asia Pacific Conference on Circuits and Systems (APCCAS)*, 2019, pp.233–236.

[22] Jagnade SA, Pandit RA and Bagde AR. Modeling, Simulation and Control of Flow Tank System. *International Journal of Science and Research* ;2015; 4: 657–669.

[23] Isidori A. 1995 'Nonlinear control system', *Springer-Verlag*, Berlin, Third Edition, pp.1–549.

[24] Boussalem c., Mansouri R, Bettayeb M. et al. Fractional order integral controller design based on a Bode's ideal transfer function: Application to the control of a single tank process. In: *Bououden S., Chadli M., Ziani S. et al (eds)* Proceedings of the 4th International Conference on Electrical Engineering and Control Applications. Springer Science Singapore Pte Ltd, 2021, pp.155–169.

[25] Chen WH and Gawthrop DJ. Optimal control of nonlinear systems: a predictive control approach. *Automatica* ;2003; 4: 633–641.

[26] Dabo M. Unconstrained NCGPC with a guaranteed closed-loop stability: Case of nonlinear SISO systems with the relative degree greater than four. In: *The 48th IEEE Conference on Decision and Control and 28th Chinese control conference*, Shanghai, China, 2009.